

Effect of Energy Restriction on Cell Cycle Machinery in 1-Methyl-1-Nitrosourea-induced Mammary Carcinomas in Rats¹

Wei Qin Jiang, Zongjian Zhu, and Henry J. Thompson²

Center for Nutrition in the Prevention of Disease, AMC Cancer Research Center, Denver, Colorado 80214

ABSTRACT

Energy restriction (ER) results in a profound inhibition of chemically induced mammary carcinogenesis. The cancer inhibitory activity of ER has been shown to be associated with lower rates of cell proliferation during both premalignant and malignant stages of this disease process. Moreover, inhibition of carcinogenesis and suppression of cell proliferation occur in animals in which plasma concentrations of insulin-like growth factor (IGF)-I are reduced, and plasma corticosterone levels are increased concomitantly. Given the role of both hormones in signal transduction pathways that can modulate cell cycle progression, albeit via different regulatory mechanisms, we report experiments conducted to determine whether hypothesized effects of changes in plasma levels of IGF-I and corticosterone on cell cycle regulation could be detected in mammary carcinomas occurring in 40% ER rats in comparison to *ad libitum* fed control rats or 40% ER rats that were energy repleted for 7 days (ER-REP). As determined by appropriate combinations of immunoprecipitations, Western blots, and kinase activity assays, it was found that levels of phosphorylated retinoblastoma and E2F-1 were significantly reduced by ER (~40 and 75%, respectively; $P < 0.01$), an effect that was partially reversed by ER-REP. Reductions in cyclin-dependent kinase (CDK)2 (82%) and CDK4 (77%) kinase activity in ER carcinomas were likely to account for the observed effects on retinoblastoma and E2F-1. Both Cip1/p21 and Kip1/p27 and levels of these proteins complexed with CDK2 were significantly elevated in ER carcinomas ($P < 0.01$), and levels of cyclin E were reduced. On the other hand, regulation of CDK4 kinase activity by ER was likely attributable to effects on cyclin D1 as well as increased binding of P16 and P19 to CDK4. The majority of changes induced by ER were reversed by ER-REP. These observations are consistent with the hypothesis that ER exerts its profound cancer inhibitory activity, in part, by multifaceted regulation of cell cycle machinery, possibly via concomitant changes in corticosterone and IGF-1 metabolism, although the role of other hormones and growth factors should not be dismissed.

INTRODUCTION

As recently reviewed (1, 2), ER³ is a potent inhibitor of experimentally induced carcinogenesis in a number of model systems, including those for breast cancer. In mammary carcinogenesis models, protection is manifested as reductions in the incidence and multiplicity of cancer and as a prolongation of cancer latency (3, 4). We have reported that under these circumstances, ER is associated with lower rates of cell proliferation and increased rates of apoptosis in both premalignant and malignant mammary pathologies (5). In the experiments reported in this study, potential mechanisms by which cell proliferation is suppressed by ER were investigated.

When ER inhibits mammary carcinogenesis, some carcinomas do

arise in restricted animals, but they are markedly smaller than the carcinomas occurring in *ad libitum* fed rats (5). We hypothesize that the same mechanism(s) that accounts for the lower incidence and multiplicity of carcinomas also accounts for the smaller size of the carcinomas that do occur and that suppression of cell proliferation is involved (5). In recently reported experiments designed to identify potential growth factors and/or hormones that mediate the effects of ER in mammary carcinogenesis, it was observed that ER is associated with a concomitant reduction in the plasma concentration of IGF-I and an elevation of plasma corticosterone (6). Given the role of IGF-I (7–11) and glucocorticoids (12, 13) in signal transduction pathways that can modulate cell cycle progression in mammary epithelial cells, we hypothesized that ER would inhibit the progression of cells through the G₁-S phase of the cell cycle. In this study, a newly reported paradigm for studying the effects of ER in a rapid emergence model for breast cancer was used to investigate in mammary carcinomas the mechanism(s) of cell cycle regulation by ER (6). Because antimitogenic effects are ultimately mediated at the level of regulation of kinases that govern transition from G₀-G₁ to S phase of the cell cycle, *i.e.*, the G₁ CDKs cyclin D-CDK4 and cyclin E-CDK2 and their respective inhibitory CKIs (11, 14), the effects of ER on these molecules and the complexes they form were investigated. The rationale for this approach is additionally strengthened by evidence that several of these cell cycle regulatory molecules have been previously identified as targets of IGF-I and/or glucocorticoids (7–13).

MATERIALS AND METHODS

Chemicals. The following materials were purchased from commercial sources: anticyclin D1, anti-CDK4, anti-CDK2, anti-P21, anti-P27, anti-P19, and anti-E2F-1 antibodies (Neomarkers, Inc., Fremont, CA); pepsin, propidium iodide, and anti- β -actin antibody (Sigma Chemical Co., St. Louis, MO); Rb-glutathione *S*-transferase fusion protein, protein A/G PLUS-agarose, anti-P16, anti-cyclin E and anti-IGF-IR antibodies, and antimouse immunoglobulin- and antirabbit immunoglobulin-horseradish peroxidase-conjugated secondary antibodies (Santa Cruz Corp. Santa Cruz, CA); histone H1 (Boehringer Mannheim, Corp., Indianapolis, IN); anti-Rb antibody (PharMingen, San Diego, CA); anti-ppAkt (phosphorylated Akt) and antitotal Akt antibodies (Cell Signaling Technology, Beverly, MA); [γ -³²P]ATP (specific activity 3000 Ci/mmol; Amersham Pharmacia Biotech, Piscataway, NJ); ECL detection system (Amersham Life Science Inc., Arlington Heights, IL).

Tissue Used for Analyses. Histopathologically confirmed mammary carcinomas used for the experiments reported herein were obtained from a previously described investigation (6). Briefly, in that study, female Sprague Dawley rats were injected with 50 mg of methyl nitrosourea/kg body weight (i.p.) at 21 days of age. After carcinogen injection, rats were randomized into one of three treatment groups: *ad libitum* fed (control); 40% energy ER continuously; and 40% ER for 6 weeks but *ad libitum* fed (ER-REP) for the last 7 days of the experiment. A modified AIN-93G diet and feeding protocol were used as described previously (15). The diet fed to 40%-DER animals was formulated to insure an intake of all nutrients equivalent to the control group, while limiting total dietary calories by reducing carbohydrate. All rats were meal fed and given two meals/day (6:00–9:00 a.m. and 2:00–5:00 p.m., 7 days/wk to avoid possible confounding because of intergroup variation of meal timing, meal number, and duration of fasting between meals).

Measurement of Adenocarcinoma Volume. Mammary adenocarcinomas were measured on the whole mount images as previously described (5), and volume was calculated using the formula $V = (\text{length} \times \text{width}^2)/2$.

Received 7/31/02; accepted 1/15/03.

The costs of publication of this article were defrayed in part by the payment of page charges. This article must therefore be hereby marked *advertisement* in accordance with 18 U.S.C. Section 1734 solely to indicate this fact.

¹ This work was supported by United States Public Health Services Grant CA52626 from the National Cancer Institute.

² To whom requests for reprints should be addressed, at Cancer Prevention Laboratory, Colorado State University, 111 Shepardson Building, Fort Collins, CO 80523-1173. Phone: (970) 491-7748; Fax: (970) 491-1044; E-mail: henry.thompson@colostate.edu.

³ The abbreviations used are: ER, energy restriction; ER-REP, energy repleted; CKI, cyclin-dependent kinase inhibitor; CDK, cyclin-dependent kinase; Rb, retinoblastoma; ECL, enhanced chemiluminescence; IGF, insulin-like growth factor; INK, inhibitor of cyclin-dependent kinase.

Analyses of Cell Cycle Distribution. Cell nuclei were dissociated from paraffin-embedded tumors histologically classified as carcinomas. Briefly, a 50- μm section of a formalin-fixed and paraffin-embedded mammary carcinoma in a small biopsy cassette was deparaffinized in xylene, hydrated gradually through graded alcohol (100, 95, 70, and 50%), and washed and soaked in distilled water. Then, the dewaxed section was transferred to a universal container with pepsin solution (0.5% pepsin in 0.9% saline with the pH adjusted to 1.5) and incubated in 37°C water bath for 30 min. After centrifuging at $800 \times g$ for 3 min and removing the supernatant carefully, the tissue fragments were resuspended, and the nuclei were released in 2 ml of PBS by agitating vigorously. Approximately 100,000 nuclei were collected by centrifugation at $800 \times g$ for 5 min and stained with 50 $\mu\text{g}/\text{ml}$ of propidium iodide, including 200 $\mu\text{g}/\text{ml}$ of RNase for 30 min and subjected to fluorescence-activated cell sorter analysis at the University of Colorado Health Sciences Center Flow Cytometry Core Facility.

RNA Isolation. Total RNA was isolated from mammary carcinomas using RNeasy Mini Kit (Qiagen, Valencia, CA) according to the manufacturer's directions. Briefly, carcinomas were homogenized using a Polytron homogenizer (Brinkman Instruments) in Qiagen RLT buffer, and cell lysate was collected by centrifugation for 3 min at $15,850 \times g$. Then the lysate was transferred onto a Qiagen-shredder column sitting in the 2-ml collection tube and centrifuged for 2 min at $15,850 \times g$. The same volume as the collected lysate of 70% ethanol was added to the homogenized lysate and mixed. The mixture was transferred to an RNeasy mini spin column sitting in a 2-ml collection tube and centrifuged for 15 s at $15,850 \times g$. After the RNeasy minicolumn was washed with Qiagen buffers RW1 and RPE, RNA was washed out from the RNeasy column with RNase-free water and collected in a 1.5-ml collection tube. The quality of total RNA was determined by measuring the absorbance at 260 nm (A^{260}) and 280 nm (A^{280}) in a spectrophotometer. The A^{260}/A^{280} ratio of samples was 1.9–2.1.

Synthesis of cDNA Probes. Total RNA was used as a template for biotinylated probe synthesis using Nonrad-GEArray Q series Kit (SuperArray, Inc., Bethesda, MD). One to 5 μg of total RNA was annealed with GEArray primer Mix at 70°C for 3 min and cooled to 42°C. Then, the RNA was labeled with labeling mixture (Nonrad-GEArray labeling Buffer, biotin-16-dUTP, RNase inhibitor, and reverse transcriptase) at 42°C for 90 min. The reaction was stopped, denatured, and neutralized by specific solutions provided by SuperArray. The resulting cDNA probe was ready to be used for hybridization.

Hybridization and Chemiluminescent Detection. GEArray Q series membrane (SuperArray, Inc.) was prehybridized with GEArray Hybridization Solution (SuperArray, Inc.) containing denatured sheared salmon sperm DNA (100 μg of DNA/ml; Life Technologies, Inc., Grand Island, NY) at 60°C for 2 h and hybridized in the Hybridization Solution (SuperArray, Inc.) containing denatured cDNA probe of the samples at 60°C overnight. After washing the membrane twice with wash solution 1 (300 mM sodium chloride, 30 mM sodium citrate, and 1% SDS) and twice with wash solution 2 (15 mM sodium chloride, 1.5 mM sodium citrate, and 0.5% SDS) for 10 min each at 60°C, the membrane was blocked in GEArray blocking solution Q (SuperArray, Inc.) for 40 min at room temperature and incubated with diluted alkaline phosphatase-conjugated streptavidin (1:5000 dilution) in buffer F (SuperArray, Inc.) for 30 min at room temperature. After the membrane was washed in a washing buffer (SuperArray, Inc.) three times and rinsed in a rinsing solution (SuperArray, Inc.), the membrane was incubated with chemiluminescent substrate and exposed to X-ray film. Signals were quantitated by scanning the film using a ScanJet scanner (Hewlett Packard), and the intensity of the spots was analyzed by using the Image-Pro Plus software (Media Cybernetics) and GEArray Analyzer (SuperArray, Inc.). β -actin and glyceraldehyde-3-phosphate dehydrogenase were used as positive controls, and bacterial plasmid (pUC18) was used as a negative control.

Expression of Cell Cycle Regulatory Molecules by Immunoprecipitation and Western Blotting. Mammary carcinomas were homogenized in lysis buffer [10 mM Tris-HCl (pH 7.4), 150 mM NaCl, 1% Triton X-100, 1 mM EDTA, 1 mM EGTA, 0.2 mM sodium vanadate, 0.2 mM phenylmethylsulfonyl fluoride, 0.5% NP40, and 0.2 units/ml aprotinin] using a Polytron tissue homogenizer (Brinkman Instruments, Westbury, NY). The lysate was collected by centrifugation for 15 min in an Eppendorf centrifuge at 4°C, and the protein concentration in the clear supernatant was determined by the Bio-Rad protein assay (Bio-Rad, Hercules, CA). Western blotting of cell cycle regulatory molecules was performed as described previously (16). Briefly, 40 μg protein

lysate/sample were denatured with SDS-PAGE sample buffer [63 mM Tris-HCl (pH 6.8), 10% glycerol, 2% SDS, 0.0025% bromophenol blue, and 5% 2-mercaptoethanol], subjected to SDS-PAGE on an 8 or 12% gel, and the protein bands blotted onto a nitrocellulose membrane (Invitrogen, Carlsbad, CA). The levels of IGF-1R, pAkt, total Akt, cyclin D1, cyclin E, cyclin A, CDK2, CDK4, P16, P19, P21, P27, E2F-1, Rb, and β -actin were determined using the specific primary antibodies designated above, followed by treatment with the appropriate peroxidase-conjugated secondary antibody and visualized by the ECL detection system. Signals were quantitated by scanning the film using a ScanJet scanner (Hewlett Packard, Palo Alto, CA), and the intensity of the bands was analyzed by using the Image-Pro Plus software (Media Cybernetics, Silver Spring, MD).

To evaluate binding of cyclin D1:CDK4, P16:CDK4, P19:CDK4, cyclin E:CDK2, P21:CDK2, P27:CDK2, and Rb:E2F-1, immunoprecipitation was performed as described previously (16). Briefly, 200 μg of protein lysate/sample were mixed with 2 μg of antibody for immunoprecipitation and 25 μl of protein A/G PLUS-agarose beads and incubated overnight at 4°C on a rocker platform. On the next day, beads were collected by centrifugation and washed three times with lysis buffer. The immunoprecipitated pellet was denatured with the SDS-PAGE sample buffer (composition given above) and subjected to 12 or 8% SDS-PAGE gel followed by Western blotting using a nitrocellulose membrane. The level of target protein was determined by specific primary antibody followed by treatment with the appropriate peroxidase-conjugated secondary antibody and visualization by the enhanced ECL detection system. Signals were quantitated by scanning the film using a ScanJet scanner (Hewlett Packard), and the intensity of the bands was analyzed by using the Image-Pro Plus software (Media Cybernetics).

Kinase Assay. CDK2 and CDK4 kinase activities were determined as described previously (16). Briefly, mammary carcinomas were homogenized in Rb lysis buffer [50 mM HEPES-KOH (pH 7.5), containing 150 mM NaCl, 1 mM EDTA, 2.5 mM EGTA, 1 mM DTT, 0.1% Tween 20, 10% glycerol, 80 mM β -glycerophosphate, 1 mM sodium fluoride, 0.1 mM sodium orthovanadate, 1 mM phenylmethylsulfonyl fluoride, and 10 $\mu\text{g}/\text{ml}$ leupeptin and aprotinin], and using anti-CDK4 antibody (2 μg) and protein A/G PLUS-agarose beads (20 μl). CDK4 was immunoprecipitated from 200 μg of protein lysate/sample as described above. Beads were washed three times with Rb lysis buffer and then once with Rb kinase assay buffer [50 mM HEPES-KOH (pH 7.5), containing 2.5 mM EGTA, 10 mM β -glycerophosphate, 1 mM sodium fluoride, 0.1 mM sodium orthovanadate, 10 mM MgCl_2 , and 1 mM DTT]. Phosphorylation of Rb was measured by incubating the beads with 40 μl of radiolabeled Rb kinase solution [0.25 μl (2 μg) of Rb-glutathione *S*-transferase fusion protein, 0.5 μl of (γ - ^{32}P)ATP, 0.5 μl of 0.1 mM ATP, and 38.75 μl of Rb kinase buffer] for 30 min at 37°C. The reaction was stopped by boiling the samples in SDS sample buffer for 5 min. The samples were analyzed by 12% SDS-PAGE, and the gel was dried and subjected to autoradiography. Similarly, CDK2 kinase activity was determined as described previously (16). Briefly, using anti-CDK2 antibody (2 μg) and protein A/G PLUS-agarose beads (20 μl), CDK2 was immunoprecipitated from 200 μg of protein in lysate/sample as detailed above. Beads were washed three times with lysis buffer and then once with kinase assay buffer [50 mM Tris-HCl (pH 7.4), 10 mM MgCl_2 , and 1 mM DTT]. Phosphorylation of histone H1 was measured by incubating the beads with 40 μl of radiolabeled kinase solution [0.25 μl (2.5 μg) of histone H1, 0.5 μl of (γ - ^{32}P)ATP, 0.5 μl of 0.1 mM ATP, and 38.75 μl of kinase buffer] for 30 min at 37°C. The reaction was stopped by boiling the samples in SDS sample buffer for 5 min. The samples were analyzed by 12% SDS-PAGE, and the gel was dried and subjected to autoradiography. Signals were quantitated by scanning the film using a ScanJet scanner (Hewlett Packard), and the intensity of the bands was analyzed by using the Image-Pro Plus software (Media Cybernetics).

Statistical Analyses. Body weight data were evaluated by ANOVA with post-hoc comparisons by the method of Bonferroni, and tumor volume data were analyzed by the Kruskal-Wallis test (17). Data derived from fluorescence-activated cell sorter analysis were evaluated by multivariate ANOVA (18). cDNA array and Western blot analyses represent semiquantitative estimates of the amount of a specific mRNA or protein, respectively, that is present in a cell extract. This fact was taken into account in the statistical evaluation of the data. The data displayed in the graphs are reported as means \pm SE of the actual scanning units derived from the densitometric analysis of each cDNA array or Western blot. All values are the means of three different experiments. However, for statistical analyses, the units of scanning

density derived from the analysis of the cDNA array or Western blots using Image Pro Plus were first ranked. This approach is particularly suitable for semiquantitative measurements that are collected as continuously distributed data. This approach has the advantage of maintaining the relative relationships among data being compared without giving undue weight to outlying results. The ranked data were then subjected to multivariate ANOVA with and without the use of tumor volume and tumor age (defined at the time in days from detection of a tumor as palpable and sacrifice of the animal in which the tumor occurred) as covariates in the analyses (18). Statistically, this is a robust approach that took into account: (a) the fact that levels and/or activities of proteins in a molecular pathway may not vary independently of one another; (b) issues that exist when multiple comparisons are being made on a particular set of data; and (c) the potential contributions of differences in tumor volume or tumor age among groups to apparent treatment-related effects.

RESULTS

Characteristics of Animals and Tumors

As noted above, tissue that was evaluated in this study was obtained from the experiment reported in Ref. 6. General characteristics of animals and tumors used in this study are summarized in Table 1. As expected, the body weights and tumor volumes of animals in the ER group were significantly lower ($P < 0.001$) than in either the control or ER-REP-treated groups. Tumor age was matched between the control and ER groups.

Effects of ER on Cell Cycle Distribution

To determine in mammary carcinomas whether the distribution of cells among the different phases of the cell cycle was affected by ER, nuclei were isolated from paraffin-embedded sections of mammary carcinomas and evaluated by flow cytometry using the approach described in "Materials and Methods." As shown in Table 2, the proportion of cells in the G_0 - G_1 phase of the cell cycle was high irrespective of treatment. Nonetheless, in comparison to *ad libitum* fed rats (control), ER resulted in a small but significant increase in the percentage of cells in G_0 - G_1 ($P = 0.050$) with concordant decreases in the percentage of cells in S phase ($P = 0.165$) and in G_2 -M ($P = 0.058$). Unfortunately, it is not possible to distinguish between cells in the G_0 versus G_1 phase of the cell cycle using this approach.

Effects of ER and ER-REP on Cell Cycle Regulatory Molecules

Gene Array Data. As an initial approach to focusing efforts to investigate the effects of ER and ER-REP on cell cycle regulatory

Table 1 Body weight, tumor age, and tumor size^a

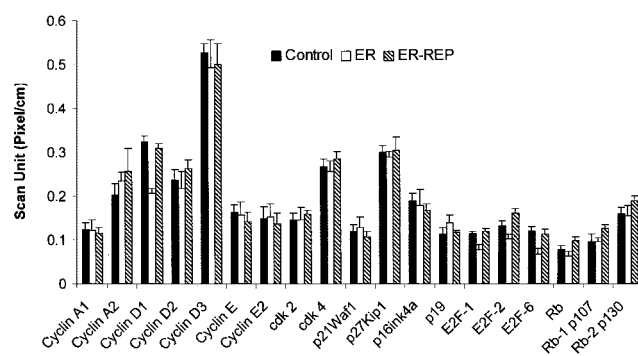
	Control	40% ER	ER-REP
Body weight (g)	184 ± 4 ^b	125 ± 1 ^c	176 ± 5 ^b
Tumor age (days)	17 ± 3 ^b	16 ± 3 ^b	8 ± 1 ^b
Tumor volume (mm) ³	283 ± 82 ^b	30 ± 10 ^c	85 ± 16 ^d
Estimated growth rate (mm) ³ /day	12 ± 3 ^b	2 ± 0.6 ^c	11 ± 0.8 ^b

^a Values are means ± SE. Values within a row with different superscripts (^b, ^c, ^d) were statistically different, $P < 0.01$. All rats were sacrificed at 75 days of age, the planned termination date of the study.

Table 2 Effect of ER on the distribution of cells isolated from mammary carcinomas in the various phases of the cell cycle^a

Cell cycle phases	Control	40% ER
G_0 - G_M1	84.9 ± 0.9	87.9 ± 1.1
S	9.8 ± 0.7	8.0 ± 1.0
G_2 -M	5.3 ± 0.6	4.1 ± 0.3

^a Each value is mean ± SE, $n = 11$ -12 carcinomas per treatment group. Data were analyzed by multivariate analysis of variance. That analysis was consistent with an increase in the percentage of cells in G_0 - G_1 phase ($P = 0.05$) and a reduction in the percentage of cells in G_2 -M ($P = 0.058$) with a statistically insignificant effect on the percentage of cells in S phase ($P = 0.165$) in ER relative to the control (*ad libitum* fed rats). The effect of energy repletion was not evaluated.



Statistical Summary of the Effect of ER or ER-REP on gene expression

Regulatory molecules	Overall multivariate statistic for an effect due to treatment with ER or ER-REP	Univariate analysis statistics (Direction of change ER vs control or ER-REP)
Cyclins	$p=0.018$	D1, decreased, $p<0.001$
Rb/E2Fs	$p=0.046$	E2F-1, decreased, $p=0.01$ E2F-2, decreased, $p=0.017$ E2F-6, decreased, $p=0.019$
CDKs and CKI	$p>0.10$	Additional analyses not warranted

Fig. 1. Gene array analysis in mammary carcinomas of rats fed *ad libitum* (control), 40% ER continuously, or 40% ER for 6 weeks but *ad libitum* until euthanized (ER-REP) as described in "Materials and Methods." Each data point is a mean ± SE of four carcinomas.

molecules, total RNA was extracted from four mammary carcinomas excised from four rats in each treatment group (control, ER, and ER-REP). A commercially available filter array was used to quantify levels of mRNA transcripts of genes involved in cell cycle regulation. The effects of these treatments are shown in Fig. 1. Because multiple endpoints were measured, the probability has increased that differences in gene expression will be found that are attributable to chance alone. To decrease this possibility, the gene expression data were divided into subgroups of genes that are known to be highly related biologically, and the data from each subgroup of genes was subjected to multivariate ANOVA. As shown in the tabular portion of Fig. 1, there was an overall effect of treatment on cyclins ($P = 0.018$) and on Rb/E2Fs ($P = 0.046$). When the strength of the multivariate analysis was considered along with the results of the univariate ANOVA generated during the multivariate analysis, the evidence indicated probable effects of ER on the D family of cyclins and members of E2F family. ER was associated with significant decreases in the expression of cyclin D1 ($P < 0.001$), E2F-1 ($P = 0.01$), E2F-2 ($P = 0.017$), and E2F-6 ($P = 0.019$). These effects were reversed in ER-REP-treated rats. No statistically significant differences were observed among treatment groups in transcripts levels of other cyclins, CDK2, CDK4, p21, p27, p16, or p19.

Cyclin D₁ and Associated Molecules. The levels of cyclin D₁, CDK4, P16, and P19 proteins in the mammary carcinomas excised from control, ER, or ER-REP-treated rats were measured by Western blotting. Because the levels of P16 were too low to detect, only results of cyclin D₁, CDK4, and P19 are shown in Fig. 2. The results of the multivariate ANOVA of these data, which are summarized in Fig. 2A, indicated a highly significant effect of dietary treatment on these proteins ($P < 0.001$). This justified additional statistical analyses of the data shown in Fig. 2B to identify the factors that accounted for statistical significance. As quantified in Fig. 2B, the level of cyclin D₁

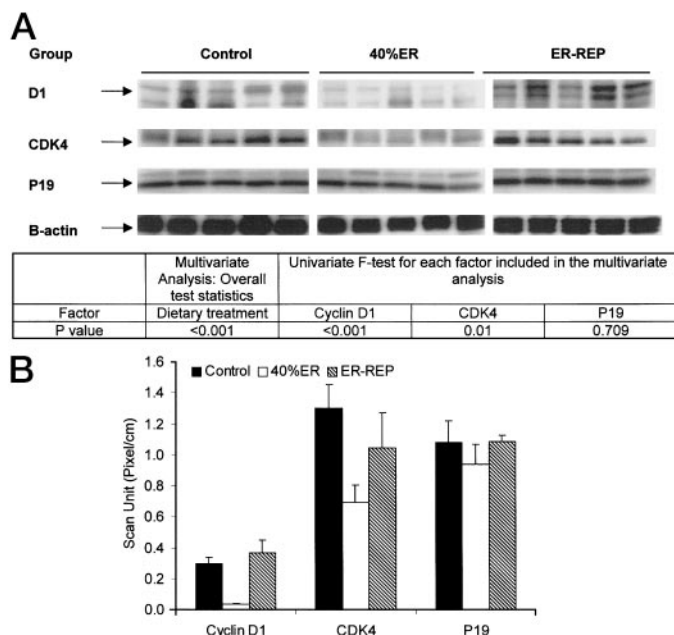


Fig. 2. Level of cyclin D1, CDK4 and P19 in mammary carcinomas of rats fed *ad libitum* (control), 40% ER continuously, or 40% ER for 6 weeks but *ad libitum* until euthanized (ER-REP) as described in "Materials and Methods." A, representative protein expression in tumor lysates determined by Western blotting as detailed in "Materials and Methods." A table of statistical analyses also is shown. B, expression data for cyclin D1, CDK4, and P19. Each data point is a mean \pm SE of 15 carcinomas.

protein was significantly lower in ER in comparison to the level in carcinomas from control (decreased 87%; $P < 0.001$) or ER-REP (decreased 89%, $P = 0.001$)-treated rats. Levels of CDK4 protein in mammary carcinomas from ER rats were significantly decreased in comparison to those in control (decreased 46%, $P = 0.001$) rats. CDK4 levels in carcinomas from ER-REP-treated rats were intermediate to those observed in carcinomas from either control or ER rats from which they were statistically indistinguishable. Levels of P19 protein among the three groups were statistically indistinguishable.

Cyclin D₁-CDK4 Complex and Associated Protein Binding. The binding of CDK4 to cyclin D1, P16 to CDK4, and P19 to CDK4 in mammary carcinomas excised from control, ER, or ER-REP rats was measured using immunoprecipitation combined with Western blotting (Fig. 3, A and B). The results of the multivariate ANOVA, which are summarized in Fig. 3A, indicated a statistically significant effect of dietary treatment ($P = 0.019$) on these protein complexes. This justified additional statistical analyses of the data shown in Fig. 3B to identify the factors that accounted for these effects. As quantified in Fig. 3B, the binding of CDK4 to cyclin D1 was lower in carcinomas from ER *versus* control-treated rats (decreased 38%, $P = 0.047$), whereas ER-REP resulted in levels of binding that were intermediate to those observed in ER and control carcinomas. The binding of P16 to CDK4 was higher in mammary carcinomas from ER rats in comparison to binding observed in carcinomas from either control or ER-REP rats (ER *versus* control: increased 1.8-fold, $P = 0.028$; ER *versus* ER-REP: increased 2.5-fold, $P = 0.028$). Binding of P19 to CDK4 was also increased by ER (ER *versus* control: increased 1.6-fold, $P = 0.028$; and ER *versus* ER-REP: increased 1.8-fold, $P = 0.016$). No statistically significant difference was observed between control and ER-REP rats in either the binding of P16 or P19 to CDK4.

Cyclin E and Associated Molecules. The levels of cyclin E, CDK2, P21, and P27 in the mammary carcinomas from control, ER, and ER-REP-treated rats were investigated by Western blotting (Fig. 4, A and B). The results of the multivariate ANOVA of these data,

which are summarized in Fig. 4A, indicated a statistically significant effect of dietary treatment on these proteins ($P < 0.001$). This justified additional statistical analyses of the data shown in Fig. 4B to identify the factors that accounted for these effects. In comparison to levels of cyclin E observed in mammary carcinomas from control or ER-REP rats, statistically significant decreases were observed in carcinomas from ER rats (ER *versus* control: decreased 85%, $P < 0.001$; and ER *versus* ER-REP: decreased 84%, $P = 0.001$). A similar effect was observed in levels of CDK2 (ER *versus* control: decreased 61%, $P = 0.001$; and ER *versus* ER-REP: decreased 59%, $P = 0.006$). Levels of P21 and P27 were increased in carcinomas from ER-treated rats (P21, ER *versus* control: increased 6.8-fold, $P < 0.001$; ER *versus* ER-REP: 4.9-fold, $P = 0.015$; P27, ER *versus* control: 3.6-fold, $P < 0.001$; and ER *versus* ER-REP: 3.4-fold, $P = 0.011$). No statistically significant differences were observed between carcinomas from control and ER-REP rats in levels of cyclin E, CDK2, P21, or P27.

Cyclin E-CDK2 Complex and Associated Protein Binding. The binding of CDK2 to cyclin E, P21 to CDK2, and P27 to CDK2 in mammary carcinomas from control, ER, and ER-REP rats is shown in Fig. 5, A and B. The results of the multivariate ANOVA of these data, which are summarized in Fig. 5A, indicated a statistically significant effect of dietary treatment ($P < 0.001$) on these protein complexes. This justified additional statistical analyses of the data shown in Fig. 5B to identify the factors that accounted for these effects. As quantified in Fig. 5B, the binding of CDK2 to cyclin E was significantly lower in carcinomas of ER rats (ER *versus* control: decreased 62%, $P = 0.009$). The binding of P21 or P27 to CDK2 was significantly higher in carcinomas from ER-treated rats relative to the control (2.2-fold increase for P21, $P = 0.009$; and 2.5-fold for P27, $P = 0.009$). Levels of each binding complex in carcinomas from

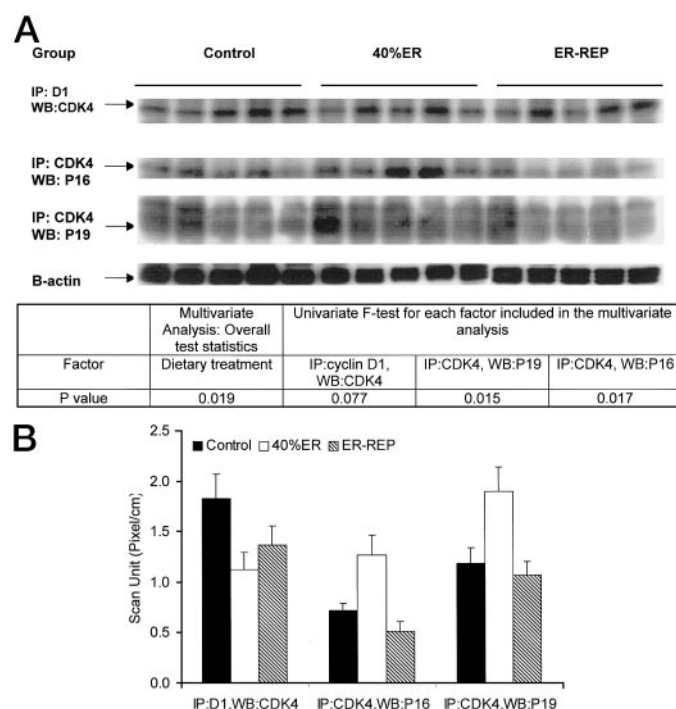


Fig. 3. Levels of cyclin D1-CDK4 complex and binding of P16 or P19 to CDK4 in mammary carcinomas of rats fed *ad libitum* (control), 40% ER continuously, or 40% ER for 6 weeks but *ad libitum* until euthanized (ER-REP) as described in "Materials and Methods." A, representative protein expression in tumor lysates determined by immunoprecipitation (IP) and Western blotting (WB) as detailed in "Materials and Methods." A table of statistical analyses also is shown. B, expression data for cyclin D1-CDK4 complex and binding of P16 or P19 to CDK4. Each data point is a mean \pm SE of 15 carcinomas.

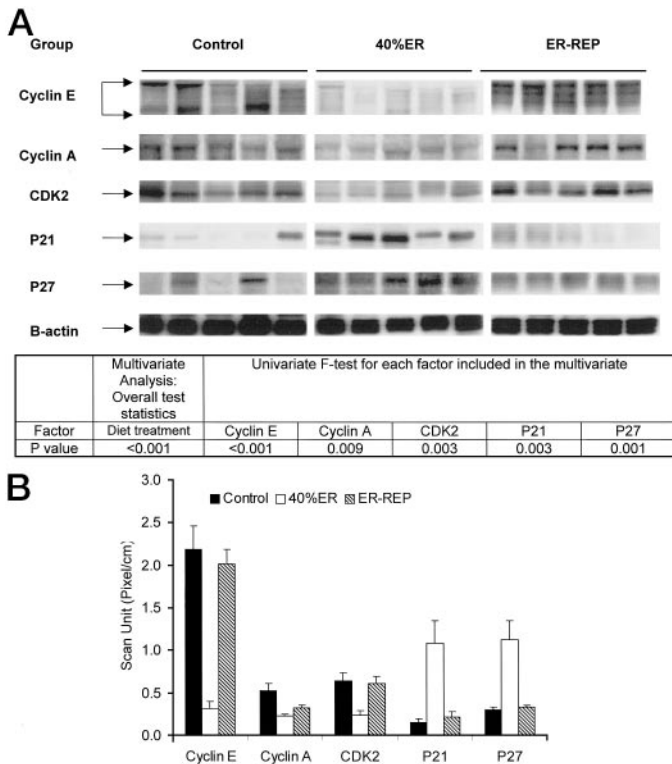


Fig. 4. Levels of cyclin E, cyclin A, CDK2, P21, and P27 in mammary carcinomas of rats fed *ad libitum* (control), 40% ER continuously, or 40% ER for 6 weeks but *ad libitum* until euthanized (ER-REP) as described in "Materials and Methods." A, representative protein expression in tumor lysates determined by Western blotting as detailed in "Materials and Methods." A table of statistical analyses also is shown. B, expression data for cyclin E, cyclin A, CDK2, P21, and P27. Each data point is a mean \pm SE of 15 carcinomas.

ER-REP-treated rats were intermediate to levels observed in carcinomas from control and ER-treated rats.

Kinase Activities and Rb/E2F-1. The CDK4 and CDK2 kinase activities, levels of hypophosphorylated and hyperphosphorylated Rb, levels of E2F-1, and the binding of E2F-1 to Rb in the mammary carcinomas from control, ER, and ER-REP treated rats are shown in Fig. 6, A and B. Multivariate ANOVA of these data (summarized in Fig. 6A) indicated a statistically significant effect of dietary treatment ($P = 0.004$) on the levels of these proteins. This justified additional statistical analyses of the data shown in Fig. 6B to identify the factors that accounted for these effects. As quantified in Fig. 6B, CDK4 kinase activity in mammary carcinomas of ER rats was significantly lower as compared with levels observed in carcinomas from control (decreased 77%, $P = 0.009$) and ER-REP (decreased 80%, $P = 0.009$)-treated rats. No statistically significant difference in CDK4 kinase activity of mammary carcinomas in control *versus* ER-REP-treated rats was observed. Statistically significant differences in the activity of CDK2 were observed among the three groups with an order of activity of ER < ER-REP < control ($P < 0.05$). Compared with ER rats, the CDK2 activity in mammary carcinomas was 5.8-fold higher in control rats and 1.9-fold higher in carcinomas of ER-REP rats.

Levels of hypophosphorylated Rb were higher, and the levels of hyperphosphorylated Rb lower in mammary carcinomas of ER-treated rats *versus* the levels observed in control or ER-REP-treated rats. A statistically significant difference was observed in the level of hyperphosphorylated Rb between ER and control treated rats ($P = 0.013$). Consequently, the ratio of hypophosphorylated to hyperphosphorylated Rb was significantly higher in mammary carcinomas of ER rats

in comparison to those of control (increased 2.9-fold, $P < 0.001$) or ER-REP (increased 2.4-fold, $P = 0.001$)-treated rats. Consistent with this pattern of response, levels of E2F-1 were significantly lower (ER *versus* control: decreased 71%, $P < 0.001$; and ER *versus* ER-REP: decreased 66%, $P = 0.002$) in mammary carcinomas of ER rats, and the magnitude of Rb binding to E2F-1 was significantly elevated in these carcinomas (ER *versus* control: increased 1.3-fold, $P = 0.047$).

IGF-IR and Akt. As an initial inquiry, two elements of a signal transduction pathway that could account for the down-regulation of cell cycle machinery regulating the G₁-S transition were investigated. Levels of IGF-IR and Akt in mammary carcinomas from control, ER, and ER-REP-treated rats are shown in Fig. 7, A and B. Multivariate ANOVA of these data indicated a statistically significant overall effect of dietary treatment on the levels of these proteins ($P < 0.001$). This justified additional statistical analyses of the data shown in Fig. 7B to identify the factors that accounted for these effects. As quantified in Fig. 7B, protein levels of IGF-IR in mammary carcinomas from ER rats were significantly lower than levels observed in control (decreased 87%, $P = 0.002$) or ER-REP (decreased 89%, $P = 0.007$)-treated rats. Statistically significant differences were also observed among three groups in the level of phosphorylated Akt with an order of ER < control < ER-REP ($P < 0.01$). Compared with ER rats, the level of phosphorylated Akt in the mammary carcinomas was increased 5.5-fold in control rats and 16.5-fold in carcinomas from ER-REP rats. Statistically significant differences were also observed in the ratio of phosphorylated Akt to total Akt between ER and control ($P = 0.024$) or ER and ER-REP ($P = 0.002$) rats, whereas no statistically significant difference was observed in the level of total Akt among the three groups.

DISCUSSION

Our laboratory has reported that ER results in the inhibition of methylnitrosourea-induced mammary carcinogenesis; this effect is

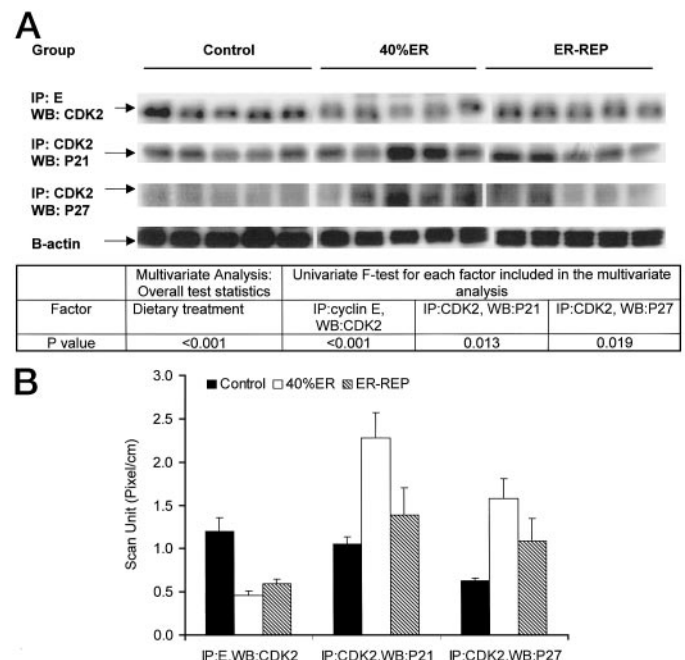


Fig. 5. Levels of cyclin E-CDK2 complex and binding of P21 or P27 to CDK2 in mammary carcinomas of rats fed *ad libitum* (control), 40% ER continuously, or 40% ER for 6 weeks but *ad libitum* until euthanized (ER-REP) as described in "Materials and Methods." A, representative protein expression in tumor lysates determined by immunoprecipitation (IP) and Western blotting (WB) as detailed in "Materials and Methods." A table of statistical analyses also is shown. B, expression data for cyclin E-CDK2 complex and binding of P21 or P27 to CDK2. Each data point is a mean \pm SE of 15 carcinomas.

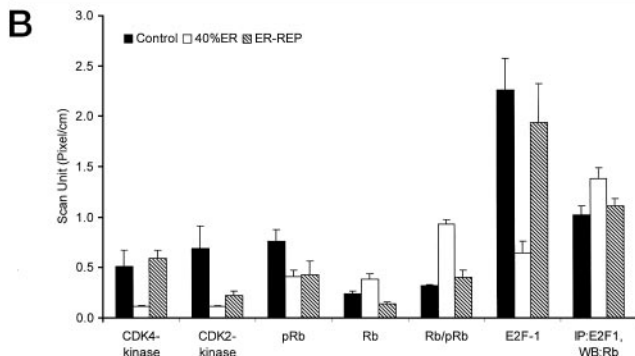
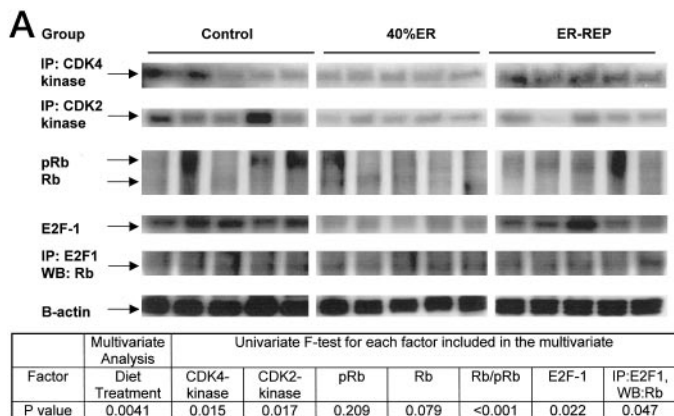


Fig. 6. Levels of CDK4 kinase activity, CDK2 kinase activity, hyperphosphorylated Rb (pRb), hypophosphorylated Rb (Rb), E2F-1, and binding of Rb to E2F-1 in mammary carcinomas of rats fed *ad libitum* (control), 40% ER continuously, or 40% ER for 6 weeks but *ad libitum* until euthanized (ER-REP) as described in "Materials and Methods." A, representative protein expression in tumor lysates determined by immunoprecipitation (IP), kinase activity assay, and/or Western blotting (WB) as detailed in "Materials and Methods." A table of statistical analyses also is shown. B, expression data for CDK4 kinase activity, CDK2 kinase activity, hyperphosphorylated Rb (pRb), hypophosphorylated Rb (Rb), E2F-1, and binding of Rb to E2F-1. Each data point is a mean \pm SE of 15 carcinomas.

manifest not only as a lower incidence and number of mammary carcinomas but also as carcinomas that have smaller mass than observed in control animals (5, 15). The smaller size with similar age of these carcinomas shown in Table 1 is consistent with an earlier report that the proliferative index determined by BrdUrd labeling is reduced by ER (5), as well as the data in Table 2 indicating that ER carcinomas have a greater percentage of cells in the G₀-G₁ phase of the cell cycle. Collectively, these data provided a strong rationale for the experiments reported in Figs. 1–7 that were designed to investigate the effects of ER on cell cycle molecules involved in regulating progression through G₁ into S phase.

As recently reported, the inhibitory effect of ER is rapidly lost when animals are released from ER (6). This observation led to the development of an experimental protocol that was used in this study to investigate the mechanisms by which ER inhibits mammary carcinogenesis. Thus, in interpreting the results shown in Figs. 1–7, it was anticipated that the effects of ER on cell cycle regulatory molecules would be reversed by the 7-day release from ER experienced by animals assigned to the ER-REP group. As an initial test of this idea, cDNA microarrays were used to evaluate whether changes in transcript levels of genes involved in the regulation of the G₁-S transition were modulated by ER and ER-REP relative to levels of expression observed in carcinomas from control animals. The results of those analyses (Fig. 1) provided compelling evidence that transcript levels of cyclin D1 and of E2F gene family members were down-regulated by ER and that these effects were reversed by ER-REP. Such effects were consistent with a delay in cell cycle progression through G₁ into

S. To additionally explore these findings, the remainder of the experiments conducted involved the measurement of differential patterns of expression of specific proteins and protein complexes involved in regulating this phase of the cell cycle. The rationale for this approach was based on the fact that the presence of a given RNA transcript does not guarantee the synthesis or quantitative expression of the corresponding protein or its activity, nor can transcript expression profiles predict the extent of protein molecular diversity associated with cellular, context-dependent posttranslational modifications, *e.g.*, phosphorylation, a key factor in cell cycle regulation.

As shown in Figs. 2 and 3, a dominant effect associated with ER was lower levels of cyclin D1 and CDK4 proteins. Predictably, lower levels of cyclin D complexed to CDK4 also were observed in carcinomas from ER-treated rats, and higher levels of CKIs P16 and P19 were observed to be associated with this kinase. These findings were consistent with the low level of CDK4 kinase activity observed in carcinomas from ER-treated rats in comparison to control carcinomas (Fig. 6). Concurrent with the down-regulation of CDK4 kinase activity, which is necessary for the phosphorylation of the Rb protein during early stages of G₁, reductions in levels of cyclin E, CDK2, and of cyclin E complexed with CDK2 also were observed in the carcinomas from ER-treated rats (Figs. 4 and 5). This plus the increased complexation of CKIs P21 and P27 with CDK2 (Fig. 5) were consistent with the reduced level of CDK2 kinase activity associated with ER (Fig. 6) despite the lack of effect of ER on transcript levels of these genes. The fact that these sequential events, *i.e.*, activation of the cyclin D1-CDK4 and cyclin E-CDK2, were reversed, albeit to different degrees, in the carcinomas of ER-REP-treated rats adds support to the interpretation that the effects observed were because of ER.

On the basis of the reduced levels of CDK4 and CDK 2 kinase activity, we predicted that the phosphorylation of Rb and levels of E2F1 would be reduced and levels of E2F1 bound to Rb would be higher than in carcinomas from ER animals. These predictions were

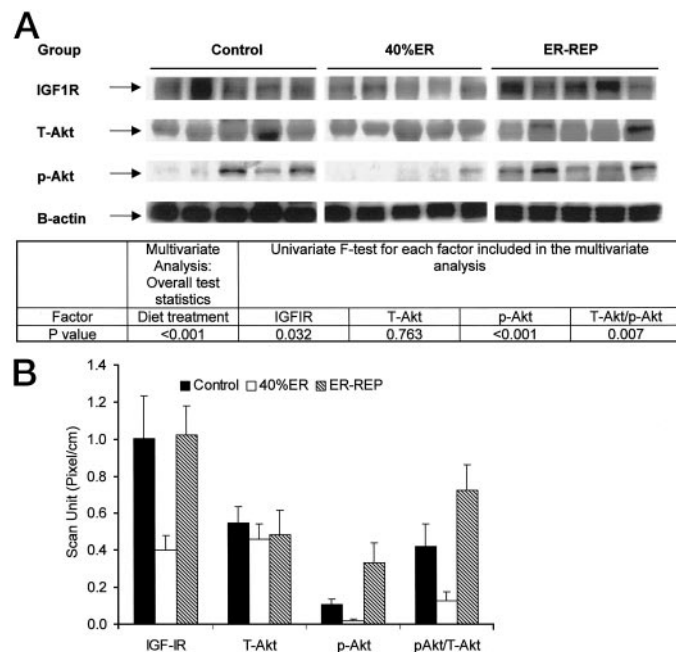


Fig. 7. Level of IGF-IR, total Akt (T-Akt), and phosphorylated Akt (p-Akt) in mammary carcinomas of rats fed *ad libitum* (control), 40% ER continuously, or 40% ER for 6 weeks but *ad libitum* until euthanized (ER-REP) as described in "Materials and Methods." A, representative protein expression in tumor lysates determined by Western blotting as detailed in "Materials and Methods." A table of statistical analyses also is shown. B, expression data for IGF-IR, T-Akt, and p-Akt. Each data point is a mean \pm SE of 15 carcinomas.

Table 3 Summary of the effects of ER on cell cycle regulatory proteins

Results of the protein expression experiments	Summaries
	<p>Levels of phosphorylated Rb and E2F-1 were significantly reduced by ER (~40 and 75%, respectively, $P < 0.01$), effects that were partially reversed by ER-REP.</p> <p>Reductions in CDK2 (82%) and CDK4 (77%) kinase activity in ER carcinomas were likely to account for the observed effects of ER on Rb and E2F-1.</p> <p>Both Cip1/p21 and Kip1/p27 and levels of these proteins complexed with CDK2 were significantly elevated in ER carcinomas ($P < 0.01$), and levels of cyclin E were reduced.</p> <p>The decrease in CDK4 kinase activity by ER was likely attributable to effects on cyclin D1 as well as increased binding of P16 and P19 to CDK4.</p> <p>The majority of changes induced by energy restriction were reversed by releasing animals from ER.</p> <p>The effects of energy restriction are consistent with multifaceted regulation of cell cycle machinery by concomitant changes in corticosterone and IGF-1, although the role of other hormones and growth factors should not be dismissed.</p>

substantiated by the data shown in Fig. 6. Moreover, as shown in Fig. 4, levels of cyclin A, which also complexes with CDK2 to maintain the phosphorylation of Rb during S phase, were reduced in the carcinomas of ER treated rats. Thus, the data in Figs. 2–6 provide a remarkably consistent picture of the down-regulation of the G₁ phase of the cell cycle attributable to ER.

As recently reported (6), concomitant changes in levels of IGF-I (decreased) and adrenal cortical steroids (increased) occur in response to ER, and these effects are reversed by energy repletion. As an initial effort to probe the chemical changes that account for reduced transit through the cell cycle, the experiments reported in Fig. 7 were conducted. We predicted that reduced levels of circulating IGF-I would be a surrogate marker for down-regulation of IGF signaling, which is mediated via the IGF-IR receptor. To explore this possibility, levels of IGF-IR protein were measured and found to be reduced by ER. Similarly, the phosphorylation of Akt, a key regulator of cell proliferation and cell survival that is affected at least, in part, by IGF-I signaling was also markedly lower in carcinomas from ER-treated rats, and the effects were partially reversed by ER-REP. Thus, it is likely that down-regulation of IGF-I pathway was involved in mediating the effects of ER on the phosphorylation of Rb. These data plus our recent reports that corticosterone induces the expression of the Kip/Cip family of CKIs, particularly P27 (6, 12, 13, 19), suggest that the concomitant changes in circulating levels of IGF-I and corticosterone work in concert to down-regulate the cell cycle. An intriguing possibility suggested by our previous report of ER-mediated inhibition of cell proliferation in combination with the cell cycle distribution data shown in Table 2 and the CKI data shown in Fig. 4 is that ER increases of percentage of cells that exit the cell cycle into G₀. The IGF-IR and Akt data are also consistent with the induction of apoptosis by ER, a possibility under active investigation by our laboratory.

In conclusion, the results of the protein expression experiments, which are summarized in Table 3, provide compelling evidence that specific events in cell cycle progression are modulated by ER. These effects are consistent with earlier reports that IGF-I and/or adrenal cortical steroids are the mediators of the cancer inhibitory activity of ER (2, 20, 21). However, the potential effects of ER on other peptides (*e.g.*, leptin) and steroid hormones (*e.g.*, estrogen) should not be discounted and also may be involved in accounting for the profound inhibitory effects of ER on mammary carcinogenesis.

REFERENCES

- Kritchevsky, D. Caloric restriction and experimental carcinogenesis. *Hybrid Hybrids*, 21: 147–151, 2002.
- Birt, D. F., Yaktine, A., and Duysen, E. Glucocorticoid mediation of dietary energy restriction inhibition of mouse skin carcinogenesis. *J. Nutr.*, 129: 571S–574S, 1999.
- Thompson, H. J., Jiang, W., and Zhu, Z. Mechanisms by which energy restriction inhibits carcinogenesis. *Adv. Exp. Med. Biol.*, 470: 77–84, 1999.
- Kritchevsky, D., and Klurfeld, D. M. Caloric effects in experimental mammary tumorigenesis. *Am. J. Clin. Nutr.*, 45: 236–242, 1987.
- Zhu, Z., Jiang, W., and Thompson, H. J. Effect of energy restriction on tissue size regulation during chemically induced mammary carcinogenesis. *Carcinogenesis (Lond.)*, 20: 1721–1726, 1999.
- Zhu, Z., Jiang, W., and Thompson, H. J. An experimental paradigm for studying the cellular and molecular mechanisms of cancer inhibition by energy restriction. *Mol. Carcinog.*, 35: 51–56, 2002.
- Wang, D., Patil, S., Li, W., Humphrey, L. E., Brattain, M. G., and Howell, G. M. Activation of the TGF- α autocrine loop is downstream of IGF-I receptor activation during mitogenesis in growth factor dependent human colon carcinoma cells. *Oncogene*, 21: 2785–2796, 2002.
- Stull, M. A., Richert, M. M., Loladze, A. V., and Wood, T. L. Requirement for IGF-I in epidermal growth factor-mediated cell cycle progression of mammary epithelial cells. *Endocrinology*, 143: 1872–1879, 2002.
- Hamelers, I. H., Van Schaik, R. F., van Teeffelen, H. A., Sussenbach, J. S., and Steenbergh, P. H. Synergistic proliferative action of insulin-like growth factor I and 17 β -estradiol in MCF-7S breast tumor cells. *Exp. Cell Res.*, 273: 107–117, 2002.
- You, H., Zheng, H., Murray, S. A., Yu, Q., Uchida, T., Fan, D., and Xiao, Z. X. IGF-1 induces Pin1 expression in promoting cell cycle S-phase entry. *J. Cell. Biochem.*, 84: 211–216, 2002.
- Lai, A., Sarcevic, B., Prall, O. W., and Sutherland, R. L. Insulin/insulin-like growth factor I and estrogen cooperate to stimulate cyclin E-Cdk2 activation and cell cycle progression in MCF-7 breast cancer cells through differential regulation of cyclin E and p21(WAF1/Cip1). *J. Biol. Chem.*, 276: 25823–25833, 2001.
- Zhu, Z., Jiang, W., and Thompson, H. J. Effect of corticosterone administration on mammary gland development and p27 expression and their relationship to the effects of energy restriction on mammary carcinogenesis. *Carcinogenesis (Lond.)*, 19: 2101–2106, 1998.
- Jiang, W., Zhu, Z., Bhatia, N., Agarwal, R., and Thompson, H. J. Mechanisms of energy restriction: effects of corticosterone on cell growth, cell cycle machinery, and apoptosis. *Cancer Res.*, 62: 5280–5287, 2002.
- Sherr, C. J. The Pezcoller lecture: cancer cell cycles revisited. *Cancer Res.*, 60: 3689–3695, 2000.
- Zhu, Z., Haeghele, A. D., and Thompson, H. J. Effect of caloric restriction on pre-malignant and malignant stages of mammary carcinogenesis. *Carcinogenesis (Lond.)*, 18: 1007–1012, 1997.
- Zhu, Z., Jiang, W., Ganther, H. E., and Thompson, H. J. Mechanisms of cell cycle arrest by methylseleninic acid. *Cancer Res.*, 62: 156–164, 2002.
- Snedecor, G. W., and Cochran, W. G. *Statistical Methods*, Ed. 6. Ames, IA: Iowa State University Press, 1967.
- Morrison, D. F. *Multivariate Statistical Methods*, Ed. 3. New York: McGraw-Hill Publishing Co., 1990.
- Zhu, Z., Jiang, W., and Thompson, H. J. Effect of energy restriction on the expression of cyclin D1 and p27 during pre-malignant and malignant stages of chemically induced mammary carcinogenesis. *Mol. Carcinog.*, 24: 241–245, 1999.
- Kari, F. W., Dunn, S. E., French, J. E., and Barrett, J. C. Roles for insulin-like growth factor-1 in mediating the anti-carcinogenic effects of caloric restriction. *J. Nutr. Health Aging*, 3: 92–101, 1999.
- Liu, Y., Wang, W., Hawley, J., and Birt, D. F. Adrenalectomy abrogates reduction of 12-*O*-tetradecanoylphorbol-13-acetate-induced extracellular signal-regulated protein kinase activity in the epidermis of dietary energy-restricted SENCAR mice: implications of glucocorticoid hormone. *Cancer Epidemiol. Biomark. Prev.*, 11: 299–304, 2002.